LA-UR- 99-2513

Approved for public release; distribution is unlimited.

Title: LEAK-PATH FACTOR ANALYSIS FOR THE NUCLEAR MATERIALS STORAGE FACILITY

Author(s): Clint Shaffer, ITS (TSA-11)
Mark Leonard, ITS (TSA-11)

Submitted to: 1999 Safety Analysis Workshop
June 13–18, 1999
Portland, OR

Los Alamos
NATIONAL LABORATORY

LEAK-PATH FACTOR ANALYSIS FOR THE NUCLEAR MATERIALS STORAGE FACILITY

Clint Shaffer and Mark Leonard
Innovative Technology Solutions
Work performed for Los Alamos National Laboratory
(505) 872-1089
CJShaffer@itsc.com

ABSTRACT

Objective
To obtain leak-path factors for the Nuclear Materials Storage Facility (NMSF) following a postulated fire.

Workshop Topic
This paper is relevant to either the Nuclear Facility Safety Analysis topic or the Risk Management topic.

Description
Leak-path factors (LPFs) were calculated for the Nuclear Materials Storage Facility (NMSF) located in the Plutonium Facility, Building 41 at the Los Alamos National Laboratory Technical Area 55. In the unlikely event of an accidental fire powerful enough to fail a container holding actinides, the subsequent release of oxides, modeled as PuO_2 aerosols, from the facility and into the surrounding environment was predicted. A 1-h nondestructive assay (NDA) laboratory fire accident was simulated with the MELCOR severe accident analysis code. Fire-driven air movement along with wind-driven air infiltration transported a portion of these actinides from the building. This fraction is referred to as the leak-path factor. The potential effect of smoke aerosol on the transport of the actinides was investigated to verify the validity of neglecting the smoke as conservative.

The input model for the NMSF consisted of a system of control volumes, flow pathways, and surfaces sufficient to model the thermal-hydraulic conditions within the facility and the aerosol transport data necessary to simulate the transport of PuO_2 particles. The thermal-hydraulic, heat-transfer, and aerosol-transport models are solved simultaneously with data being exchanged between the models. A MELCOR input model was designed such that it would reproduce the salient features of the fire per the corresponding CFAST calculation. Air infiltration into and out of the facility would be affected strongly by wind-driven differential pressures across the building. Therefore, differential pressures were applied to each side of the building according to guidance found in the ASHRAE handbook using a standard-velocity head equation with a leading multiplier to account for the orientation of the wind with the building. The model for the transport of aerosols considered all applicable transport processes, but the deposition within the building clearly was dominated by gravitational settling.

Results
The transport of respirable PuO_2 aerosols depended most strongly on parameters that affect the rate of air infiltration into and out of the building, specifically infiltration flow areas and wind velocities. The study assumed that all doors to the outside were closed within 5 min after the initiation of the fire, well before any container holding plutonium was postulated to fail, and it did not attempt to account for infiltration other than door leakage. When reasonably small air infiltration flow rates were modeled, the predicted LPFs were substantially less than 1%. When realistic, continuous-averaged wind velocities (< 10 mph) and tightly closing doors were assumed, the predicted LPFs were generally less than 0.01%. When infiltration was eliminated, the LPF for leakage through the high-efficiency particulate air (HEPA) filters and towers was less than 0.0001%. The aerosol models used for the bulk of these calculations neglected

the soot particles associated with smoke produced by the fire. The calculations demonstrated that including smoke in the analysis reduced the predicted LPF substantially.

Benefits

The analysis provided guidance for the continuing design of the facility and illustrated analytical techniques for performing such analyses.

INTRODUCTION

Leak path factors (LPFs) were estimated for the Nuclear Materials Storage Facility (NMSF) located in the Plutonium Facility, Building 41 (PF-41) at the Los Alamos National Laboratory Technical Area 55 (TA–55) [1]. The NMSF is being designed to provide intermediate and long-term storage for actinides, a staging/storage area for weapon components, a centralized shipping/receiving facility for nuclear materials, and laboratory space for the nondestructive assay (NDA) work associated with shipping, receiving, and storing actinides. Actinides will be received in the form of metals, oxides, and pits in containers.

In the unlikely event of an accidental fire powerful enough to fail a container holding actinides that released oxides (PuO_2 aerosols) into the facility, the subsequent release of those oxides out of the facility and into the surrounding environment must be predicted. One aspect of these predictions is the estimate of the LPF, defined here as the fraction of the respirable oxide that was released into the facility and that subsequently was released into the environment. The LPF estimates varied with the postulated accident conditions and modeling assumptions used.

The postulated accident conditions modeled in the analysis described here included the following features.

- A 1-h fire is located in the NDA laboratory on the main floor of the facility.
- The actinides are initially inside a container that fails as a result of sustained heating by the fire (at 20 min or greater).
- The automatic sprinkler protection systems do not operate.
- The ventilation system fans are not operating, and the system dampers fail open.
- The facility doors to the outside are closed within 5 min, well before any actinide is released into the facility.
- A wind blows across the building approaching from the north side where the truck loading/unloading bay is located. This wind creates a small pressure differential across the building that forces air infiltration through the building.
- The quantity of actinides released is small, so coagulation of smaller particles into larger particles is not significant. (Therefore, the calculated LPFs are conservative for large releases.)

Smoke aerosols were neglected in the base calculations, but additional calculations were run to verify that neglecting smoke was conservative, i.e., that modeling smoke would reduce the LPF values. The calculations that modeled smoke also clearly illustrated the substantial potential effect that smoke could have on enhancing actinide deposition within the facility.

The LPFs were calculated using the MELCOR nuclear power plant severe accident analysis code. Although MELCOR was developed to simulate the meltdown of a nuclear reactor, the code is readily adaptable to nonreactor analysis through user input without any modifications.

OVERVIEW OF MELCOR

The MELCOR code, which was developed at Sandia National Laboratories for the U. S. Nuclear Regulatory Commission, is a fully integrated computer code that models the progression of severe accidents in light-water-reactor nuclear power plants [2]. The entire spectrum of severe accident phenomena, including the reactor coolant system and the containment thermal-hydraulic response; nuclear core heatup, degradation, and relocation; and fission-product release and transport, is treated in MELCOR in a unified framework for both boiling- and pressurized-water reactors.

The thermal-hydraulic behavior is modeled with a lumped-sum approach using control volumes connected by flow paths. Each volume is defined spatially by its volume vs altitude; it may contain a gravitationally separated pool of single- or two-phase water and an atmosphere consisting of any combination of water vapor, suspended water droplets, or noncondensible gases. The flow paths connect volumes and define paths for moving hydrodynamic materials. The governing thermal-hydraulic equations are the equations of conservation of mass, momentum, and energy. The transfer of heat between control-volume atmospheres and pools and their surrounding surfaces is modeled using one-dimensional heat structures. In this study, the heat structures were used to model the room walls, floors, and ceilings.

MELCOR contains models to predict the transport and behavior of radionuclide vapors and aerosols that directly couple to the thermal-hydraulic models. Radionuclide aerosols and vapors may deposit directly on surfaces such as heat structures and water pools, and aerosols may agglomerate and settle. The particle coagulation processes modeled include Brownian diffusion, gravitational settling, and turbulent impaction. The aerosol deposition processes modeled include gravity, diffusion, thermophoresis, and diffusiophoresis.

MELCOR INPUT MODEL

The input model for the NMSF consists of a system of control volumes, flow pathways, and surfaces sufficient to model the thermal-hydraulic conditions within the facility and the aerosol transport data necessary to simulate the transport of PuO_2 particles. The thermal-hydraulic, heat-transfer, and aerosol-transport models are solved simultaneously with data being exchanged between models.

Facility Nodalization. With a few exceptions, each room within the facility was treated as a separate control volume and each doorway was treated as a separate flow pathway. Corridors on the main floor and the charge hall were subdivided further to better model aerosol transport within them. The main floor NDA laboratory also was subdivided further into seven smaller volumes to better model the fire as discussed below. After the aerosol transport to and from the basement level and to and from the support area was determined to be relatively minor, several of those rooms were combined into singular volumes to facilitate the overall solution. The nodalization scheme for the calculations documented here is shown in Figs. 1 and 2 for the main and basement levels, respectively.

Surfaces. Room surfaces were modeled primarily to provide locations for aerosol deposition. The areas associated with equipment and office furniture were not modeled. Surfaces were oriented as floors, walls, or ceilings because orientation is important to gravitational deposition. The MELCOR models treat gravitational deposition onto floors but not onto ceilings or walls. Other forms of deposition are treated for all orientations. The surface heat transfer to or from volume atmospheres was treated as well, such as the NDA laboratory where substantial heat was radiated directly to the walls.

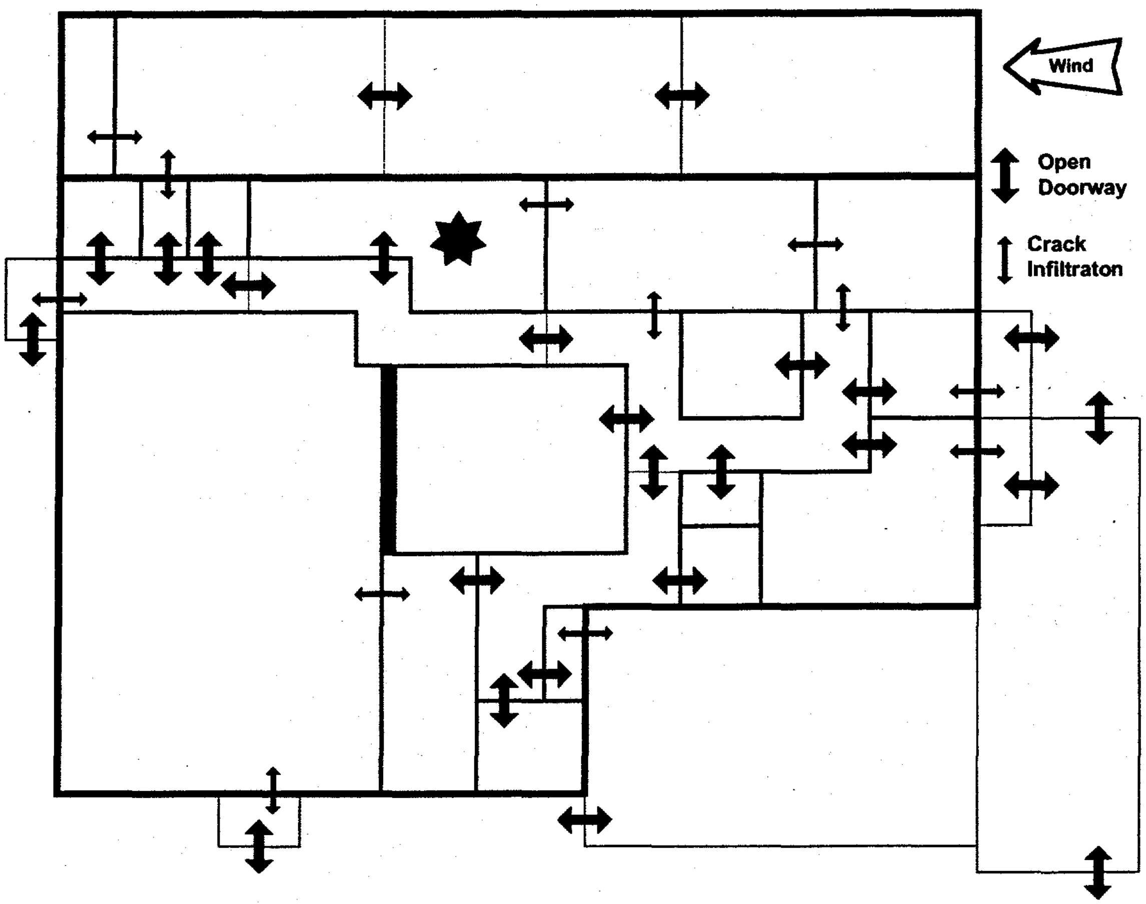

Fig. 1. Nodalization of the Main Level.

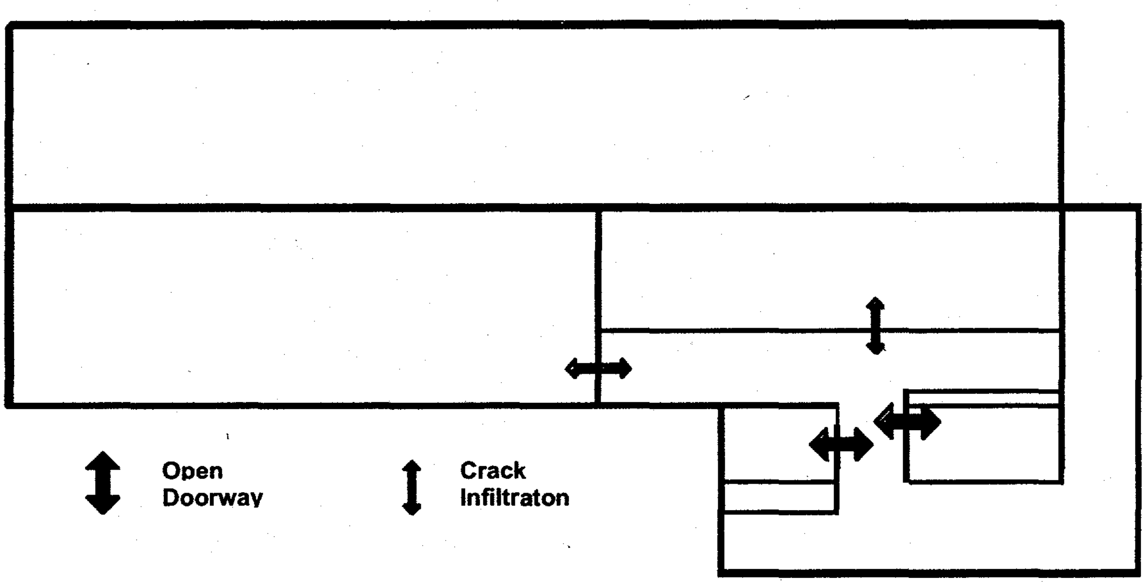

Fig. 2. Nodalization of the Basement Level.

Building Transport Pathways. Flow pathways between the main and basement levels include the stairwell, the elevator shaft, and the ventilation systems. The stairwell was modeled as a singular volume with its floor at the basement level and its ceiling at the main level; the doors were assumed to be at least partially open. The elevator shaft pathway from the basement level to the main level assumes a small gap around the elevator car perimeter. The ventilation systems are discussed below.

Of the vast number of possible door configurations possible, only one configuration was modeled in these calculations. The doors were first classified as either on a differential pressure zone boundary or interior to a zone. Note that the differential pressure zones occur when the ventilation systems are operating and are intended to transfer air from areas of low probability of contamination to areas of higher probability of contamination by maintaining slightly lower pressures in the areas of higher probability such as the NDA laboratory. The rational for separating the doors into two types is that the pressure boundary doors are likely to have better seals than the other doors. For example, an office door usually has a substantial gap beneath it so that even if the door is closed, air can bypass the door carrying aerosols with it. The two types of door pathways can be distinguished in Figs. 1 and 2 by the size of the two-way arrow indicating the door. The flow, as modeled, can move in either direction depending on the relative differential pressures. All non-zone doors were modeled as open, and all zone boundary doors except one NDA laboratory door to the corridor were modeled as closed.

Air infiltration into and out of the facility and across zone boundaries was modeled as "cracks" around the door perimeters to provide the proper resistance to flow. Note that other potential sources of air infiltration, such as walls, were not modeled. Each door crack was assumed to have a flow area equivalent to one-half of the door perimeter, and a specified gap (variable in the parameter sensitivity calculations), and a flow-loss coefficient of 2.7.

Ventilation Systems. Facility ventilation systems were modeled in the passive mode, i.e., the fans were not operating and the dampers were open. These systems included the air recirculation system, the air makeup supply system, and the air exhaust system.

The recirculation system consists of two high-efficiency particulate air (HEPA) filter units and two fans located in the heating, ventilating, and air conditioning (HVAC) mechanical equipment room and associated ducting to rooms on both the main and basement levels. The MELCOR input model consists of eight control volumes and connecting pathways, as shown in Fig. 3, that simulate the HEPA filter plenums and air ducts. The two HEPA filter units were combined into a single unit in the MELCOR model. Note that the exhaust registers in each room are located at the floor and the supply air diffuses at the ceiling level. Although the direction of flow shown in Fig. 3 corresponds to flows with the fans operating, the flows in the MELCOR simulation could move in either direction depending on the differential pressures associated with air infiltration and natural circulation. The ducts were subdivided into three main trains in an attempt to crudely simulate the actual duct layout. Although this model was necessarily somewhat crude, it does contain the salient features of the system, i.e., natural circulation through the HEPA filter between exhaust and supply registers and natural circulation flow between rooms on the same duct train, such as between the NDA laboratory and the packing/unpacking room. Each volume has a surface area that allows aerosol deposition to occur inside the ventilation ducting.

The facility makeup air and exhaust systems are connected directly to the outside through HEPA filters and the towers. The MELCOR input model is shown in Fig. 4. Because the exhaust tower is higher than the supply tower and the air temperatures within each tower may differ, some natural circulation between the facility and the outside is likely and the MELCOR model did simulate this circulation. Duct surfaces, and therefore gravitational settling, were not simulated in this model. Again, flows can move in either direction depending on differential pressures.

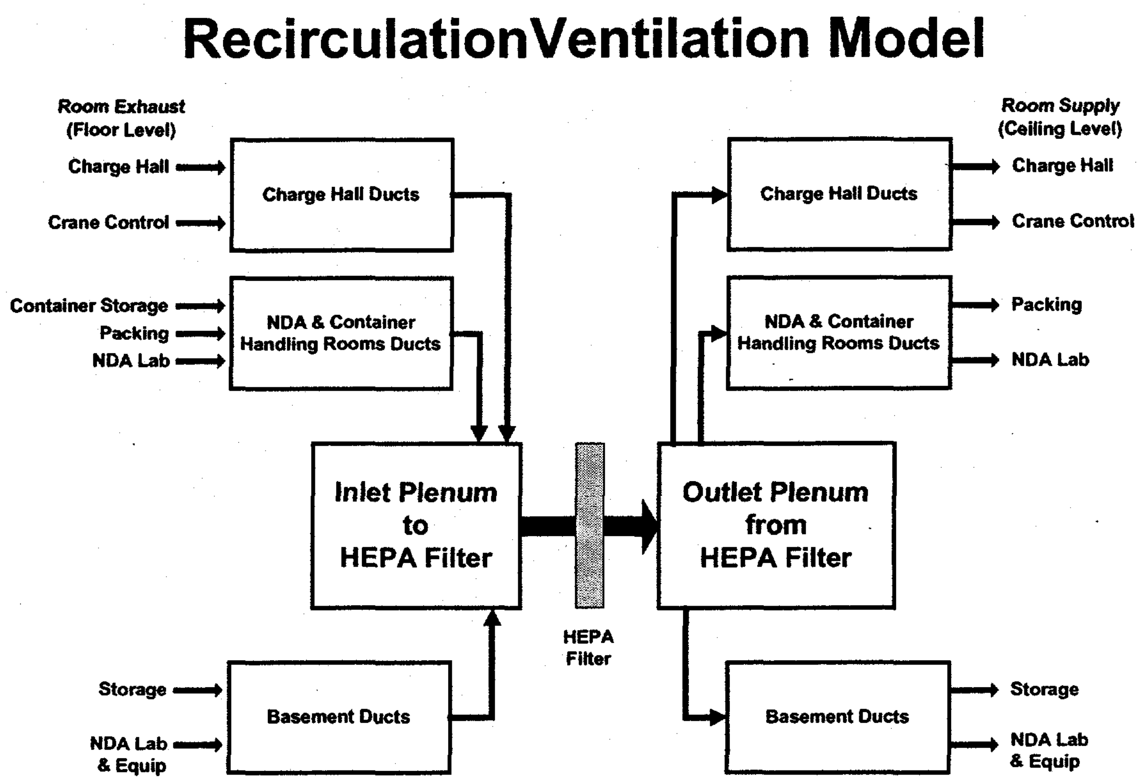

Fig. 3. Nodalization of the Ventilation Recirculation System.

The flow-loss coefficients for the HEPA filters were based on data the Nuclear Aircleaning Handbook [3]. It gives a head loss of 1 in. H_2O at 1000 ft^3/min for a HEPA filter measuring 2 ft by 2 ft by 1 ft deep. The loss coefficient corresponding to this head loss is 256.

Fire Model. All simulations here assumed a 1-h fire in the NDA laboratory on the main floor. A MELCOR input model was designed such that it would reproduce the salient features of the fire per the corresponding CFAST calculation [4]. Note that although MELCOR does have models for hydrogen combustion within reactor containments, it does not have models to simulate the burning of the combustible materials found in the NDA laboratory.

The salient parameters of the CFAST calculations were as follows.

- A fuel loading of 864 lbm of combustible materials (~1 lbm/ft^2).
- An energy release of 8000 Btu/lbm.
- The entire fuel load was assumed to burn over the initial 2700 s (2560 Btu/s) with a subsequent ramp to zero at 3600 s.
- One NDA door is open.
- A maximum plume temperature of 755°F.
- Supply airflow to the fire of 3.4 lbm/s.
- The neutral plane between cool air entering the NDA laboratory through the open door and hot gases leaving through the same door was 2.8 ft above the floor.
- A fire plume accumulates in the laboratory space above the top of the door.

Makeup Air Ventilation Model

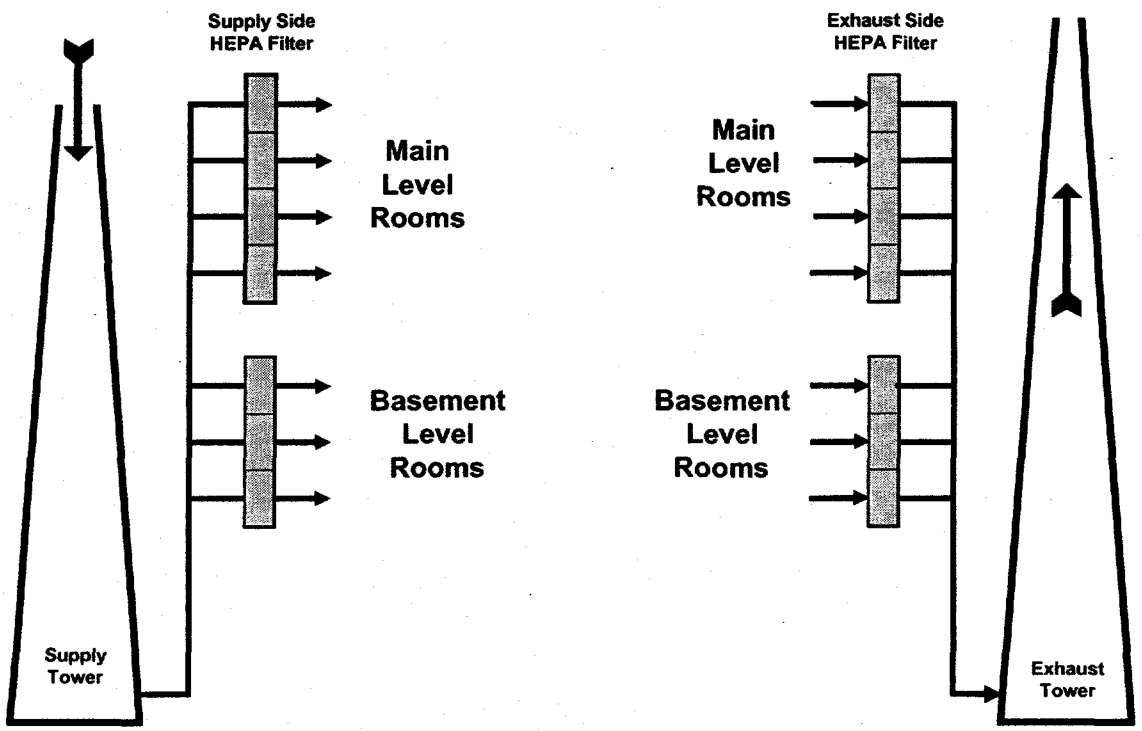

Fig. 4. Nodalization of the Facility Makeup Air and Exhaust Systems.

Additional considerations needed to appropriately model the aerosol transport are the flow velocities in the NDA laboratory and the air circulation in the adjoining hallway. Flow velocities strongly affect aerosol residence times within the NDA laboratory and the their subsequent deposition. Relatively high flow velocities would be expected directly above the fire and between the fire and the doorway, but considerably slower velocities would be expected in the portions of the laboratory away from the fire and the door. Substantial deposition could occur because of gravitational settling from the fire plume to slower back areas of the room. The MELCOR input model, which is shown in Fig. 5, attempted to simulate these velocities. The model has three levels associated with the door flow, i.e., the cool air entering at the bottom of the door, the hot gases leaving at the top of the door, and the fire plume above the door. The flow into the door was fixed at the desired flow rate until the fire went out, then the flow rate tapered off while the room cooled. Both heat and aerosol particles were introduced into the center column that simulated the fire itself. The space between the fire and the doorway was modeled with three vertically stacked, relatively small volumes, and the remainder of the room was modeled by three vertically stacked, relatively larger volumes. The code automatically relocated aerosol particles that settled out in one of the upper volumes into the volume below it. The anticipated velocities and aerosol deposition were obtained successfully.

It was necessary to subdivide the NDA corridor into levels to move the hot gases away from the laboratory door; otherwise an unrealistic reentry of hot gases into the laboratory occurred, resulting in some exceptionally high temperatures. A two-layer model was used with the division set at a level 2.8 ft above the corridor floor, corresponding to the CFAST-predicted neutral plane. This scheme is shown in Fig. 6. In reality, hot

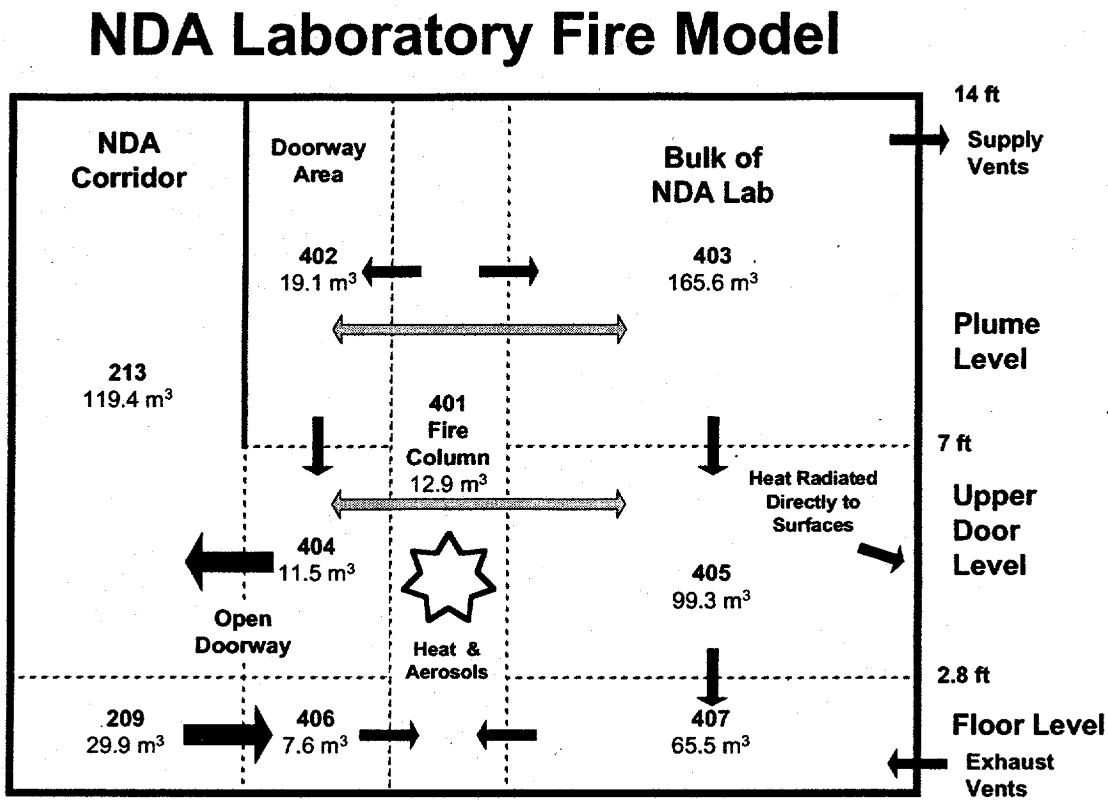

Fig. 5. Nodalization of the NDA Laboratory.

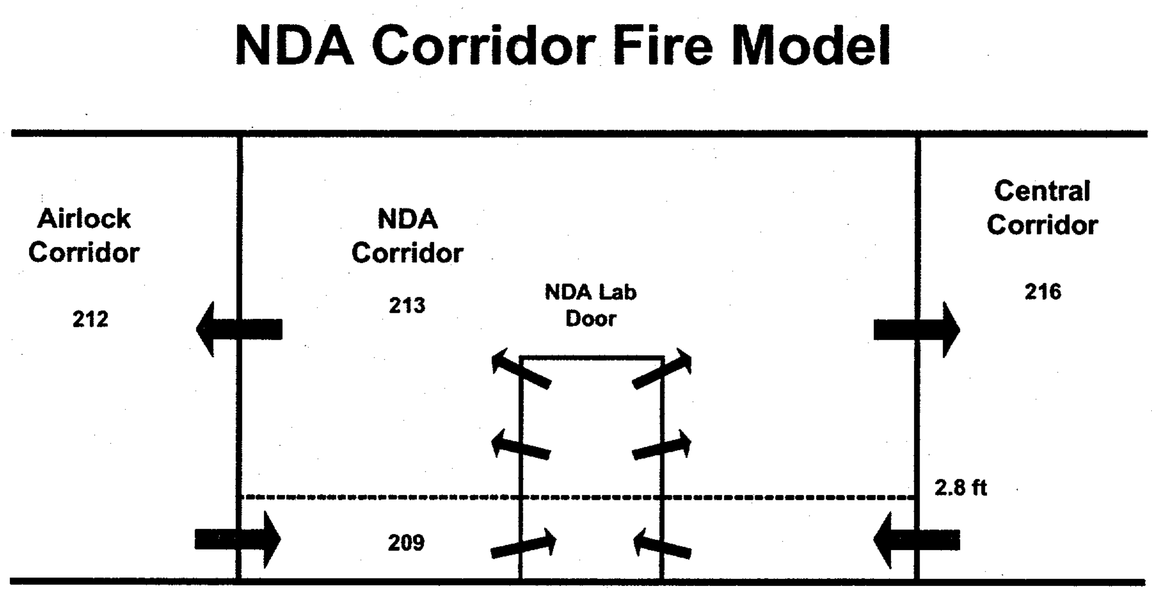

Fig. 6. NDA Corridor Model.

gases and smoke from the fire would tend to rise to the top of the corridors above the door tops and flow along the corridors to their far ends before significant hot gases enter the adjoining rooms. Therefore, the NDA corridor split-layer input model tends to predict the correct trends.

Obtaining temperatures within the NDA laboratory characteristic of the simulated fire was important to the aerosol deposition processes. These temperatures do not need to be modeled exactly, just reasonably close to the characteristic temperatures. Initial modeling efforts showed unrealistically high temperatures if all of the heat was dumped directly into the laboratory air. In reality, a significant fraction of the fire heat would radiate directly to surrounding surfaces. Therefore, the MELCOR model was modified to source a fraction of the heat directly onto the surfaces using a plausible distribution. This fraction then was adjusted until the laboratory air temperatures peaked near the desired 755°F. As it turned out, 80% of the total heat was placed directly into the concrete surfaces, and 20% was put into the air. Although CFAST predicted only 30% of the total heat radiated directly to the walls, the important consideration for aerosol transport is that the correct temperatures were achieved. In any case, heat absorbed by the walls was largely transferred back to the laboratory air after the fire ended.

Meteorological Conditions. Air infiltration into and out of the facility would be affected strongly by wind-driven differential pressures across the building. For the calculations reported here, the wind was modeled as coming from only the northern direction, i.e., into the building on the truck loading/unloading side. Differential pressures were applied to the building using separate environmental control volumes for each side of the building, i.e., the front, back, and sides. A fourth environmental volume with standard atmospheric pressure was used for the entrance/exit of the towers. The differential pressures across the building were set according to guidance found in the ASHRAE handbook [5] using a standard-velocity head equation with a leading multiplier to account for the orientation of the wind to the building. The values used for coefficient C were 1.2 for the pressure drop from the front to the back of the building and 1.0 for the front to the sides of the building.

All of the calculations that were run except one assumed a steady-state wind velocity through the duration of the calculation. The exception assumed the wind was gusting with the gust wind velocities predicted using a cycling trigonometric function.

Aerosol Transport Input Models. In setting up an aerosol transport model, the process (or processes) likely to dominate the aerosol transport for the aerosol characteristics and the expected thermal-hydraulic conditions should be determined first. An evaluation clearly showed that gravitational settling is dominant for particles larger than about 0.3 µm and diffusion dominates for particles smaller than 0.3 µm.

Aerosol Source. MELCOR does not model the generation of aerosol particles for this type of application; therefore, the postulated NDA laboratory aerosols were simply introduced as a source into the volume representing the fire. The parameters required to specify the source include the particle-size distribution, the quantity, and the timing of release. Because the focus of this study was respirable PuO_2, a size distribution was selected that focused on particles smaller than about 3 µm. The base-case distribution selected was a 2-µm mass medium diameter (MMD) lognormal distribution with a standard deviation of 2. Approximately ~75% of this distribution is smaller than 3 µm. An alternative distribution of 1-µm MMD was examined as a sensitivity case.

The source was introduced as a burst release at 20 min to simulate the failure of a container because of fire heating. Because the timing of the failure is not known, an alternate failure time of 40 min was examined as a sensitivity case.

The quantity of aerosol introduced was kept small to prevent significant particle coagulation. The coagulation of smaller particles into larger particles would enhance deposition and strongly depends on the density of particles. Without coagulation, the LPFs obtained for a small particle densities can be applied conservatively to larger particle densities. The source quantity here was always 1 g.

Several aerosol transport parameters require specification in the MELCOR models. Because gravitational deposition dominated the transport results, the variables of particular interest are the particle density and the dynamic shape factor. Most of the calculations were run using a shape factor of either 1.0 or 1.2, and the density was specified as 11,000 kg/m^3. The calculational sensitivity of these parameters was deemed to be less significant than the specification of the size distribution.

A HEPA filter filtration efficiency of 99.98% was used for most of the calculations. This efficiency reflects the fact that some of the particles in the sub-micron range will slip through the filter. One sensitivity calculation was run to examine the importance of accurately knowing this efficiency.

Soot particles are much lighter and therefore tend to settle slower than PuO_2 particles the same sized, but the much larger particle density of smoke causes the soot to coagulate into substantially larger chains of particles that will settle faster than smaller particles. Soot coagulation will trap PuO_2 particles in the larger soot chains. In the calculations that modeled soot as well as PuO_2, a two-component aerosol model was used that allowed a distinction between the two types of aerosol particles. Because the density of smoke far exceeded the density of PuO_2, the transport parameters common to both components were specified for soot. Because soot aerosol particles tend to be long chains of smaller particles, a larger dynamic shape factor was used than was used for PuO_2 alone. Because the two-component model only allowed one solid particle density (set at 100 kg/m^3 for soot), the PuO_2 diameter was adjusted to obtain a velocity deposition rate somewhat less than that of the single-component, PuO_2-alone model per the gravity deposition equation.

CALCULATIONAL RESULTS

A series of calculations was run to estimate the LPFs for the 1-h NDA laboratory fire accident scenario for a variety of conditions and input parameter selections. The LPF depends on the value assumed for a number of parameters. The parameters that were varied included the following.

- The wind velocity and whether the wind is steady state or transient
- The flow area for air infiltration into and out of the facility
- The container failure time
- The particle shape factor
- The HEPA filter particle collection efficiency
- The smoke aerosol density (if modeled)

These variations and their predicted LPFs are listed in Table 1. Recall that the LPF calculated here is defined as the fraction of the respirable oxide that was released into the facility that subsequently was released into the environment.

Base Case. Calculation 2 is considered the base case in these calculations. Case 2 included the ventilation system model and assumed that the container failed at 20 min thereafter, releasing a PuO_2 aerosol in the NDA laboratory with a size distribution characterized by MMD of 2 μm, a standard deviation of 2, and a shape factor of 1.2. The facility air infiltration was driven by a steady-state, 30-mph wind through flow areas modeled as a 0.5-mm crack over one-half of the door perimeters. The HEPA filters trapped 99.98% of all aerosols passing through the filters; smoke aerosols were neglected. These input parameters resulted in a predicted LPF of 0.0039; i.e., 0.39% of the initial aerosol released into the

Table 1. Results of MELCOR LPF Calculations

Case	Vent. Model	Container Failure Time	Aerosol Size (MMD)	Shape Factor	Crack Width	Wind Speed	Wind Gusting	HEPA Collect Eff.	Smoke Density	Leak Path Factor
		Min	Micron		mm	mph			kg	
0	**none**	20	2	**1**	0.5	30	steady	-	none	7.0E-03
1	passive	20	2	**1**	0.5	30	steady	99.98%	none	2.9E-03
2	**passive**	**20**	**2**	**1.2**	**0.5**	**30**	**steady**	**99.98%**	**none**	**3.9E-03**
3	passive	20	**1**	1.2	0.5	30	steady	99.98%	none	1.0E-02
4	passive	**40**	2	1.2	0.5	30	steady	99.98%	none	5.6E-03
5	passive	20	2	1.2	**0**	30	steady	99.98%	none	1.4E-07
6	passive	20	2	1.2	**1**	30	steady	99.98%	none	9.3E-03
7	passive	20	2	1.2	**2**	30	steady	99.98%	none	2.0E-02
8	passive	20	2	1.2	0.5	**10**	steady	99.98%	none	**1.1E-04**
9	passive	20	2	1.2	0.5	**20**	steady	99.98%	none	1.0E-03
10	passive	20	2	1.2	0.5	30	**gusty**	99.98%	none	4.4E-03
11	passive	20	2	1.2	0.5	30	steady	**99.95%**	none	3.9E-03
12	passive	20	2	1.2	0.5	30	steady	99.98%	**10**	**2.6E-05**
13	passive	20	2	1.2	0.5	30	steady	99.98%	**25**	1.1E-05
14	passive	20	2	1.2	0.5	30	steady	99.98%	**50**	5.9E-06
15	passive	20	2	1.2	**5**	30	steady	99.98%	none	5.1E-02
16	passive	20	2	1.2	0.5	**1**	steady	99.98%	none	2.8E-07
17	passive	20	2	1.2	0.5	**10**	steady	99.98%	**25**	**1.4E-07**

NDA laboratory subsequently was released into the environment. Selected detailed results of Case 2 are discussed to provide a better feel for the general performance of the calculations.

The calculations continued until the aerosols were either deposited onto a surface or transported to the environment. After aerosol particles were deposited, the aerosol could not be resuspended. This condition was determined by monitoring the aerosol still airborne within the facility. The calculations usually were terminated at 18 h. Figure 7 shows the mass of aerosol still airborne, the mass deposited on surfaces within the facility, and the mass escaping to the environment.

As expected, the larger particles fell out faster than the smaller ones; thus, the size distribution of the remaining airborne particles becomes increasingly smaller.

Gravitational settling was verified as the dominant deposition mechanism. About 87% of the deposits were on the floor compared with 0.5% on the ceiling and about 13% on the walls. In MELCOR, gravitational settling to a ceiling is actually a negative deposition process, whereas the walls are neutral and the floor is positive. Therefore, deposition occurring on the walls would be primarily a result of the diffusion mechanism. The total floor and ceiling surface areas were nearly the same; the wall surface area was more than twice that of the floors.

It is insightful to look at the final aerosol deposition distribution within the facility to determine if the distribution seems reasonable. A reasonable distribution adds to the credibility of the calculation. The final distribution for Case 2 is shown in Table 2.

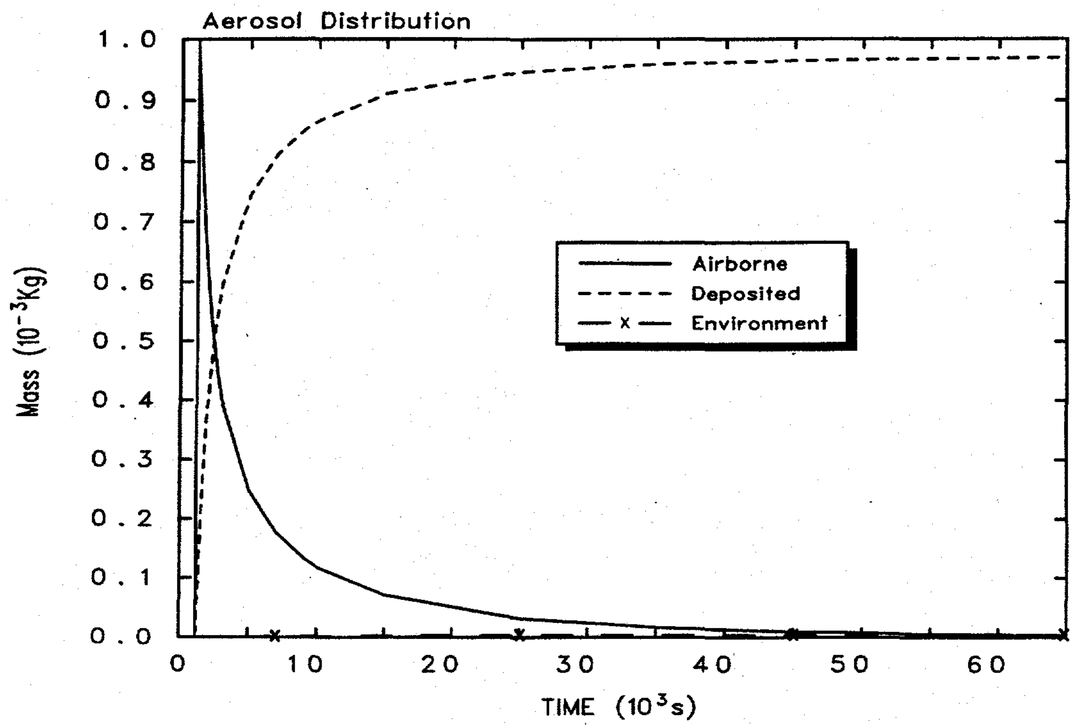

Fig. 7. Timing of Aerosol Transport.

Table 2. Final Distribution of Aerosols

Location	**Percentage**
NDA Laboratory	21.21%
NDA Corridor	13.65%
Central Corridor	22.05%
X-Ray Corridor	6.19%
Packing/Unpacking	10.01%
Charge Hall	4.18%
Remainder of Main Floor	7.23%
Ventilation Ducts	9.47%
Filters	1.81%
Basement	3.26%
Support Area	0.55%
Environment	0.39%
Total	100.00%

The advantage of subdividing the NDA laboratory to more accurately depict the flow velocity across the room is reflected in the result that 21% of the aerosols were predicted to remain in the room, and this seems to be a reasonable result. The velocities at or near the fire were on the order of 2.5 m/s while the fire was burning but only a few tenths of a meter per second in the bulk of the room away from the fire. Experience has shown that if a single-volume model had been used, the aerosols would have been largely swept out of the room. The importance of the split-layer corridor model is reflected in the result that the deposition in the NDA corridor and its two adjoining corridors was about 42%. This is physically realistic because the smoke would tend to be trapped in the corridors above the tops of the doors. The result of 10% of the aerosol being deposited in the packing/unpacking room was perhaps less expected because the door connecting the two rooms was closed. As it turns out, there was a substantial natural circulation path established in the ventilation ducting because both the NDA and the packing/unpacking room were on common ducts. Thus, the ductwork flow behaved as through there was a hole at both the top and bottom of the adjoining wall. A similar but smaller connection existed between the NDA laboratory and the charge hall and between the NDA laboratory and the basement.

The temperatures in the NDA laboratory and the adjoining corridors are shown in Fig. 8. The peak temperature for Case 2 was 685°F compared with 755°F for the CFAST calculation. Although the model could have been adjusted further, this result was deemed accurate enough for the purposes of this calculation. Note that the mid-height wall-surface temperature lags behind the air temperature during the fire but then continues to heat the room well after the fire has gone out. The two corridor temperatures reflect the hotter gases leaving the laboratory at the top of the door and the warm but colder temperature of the air entering at the bottom of the door.

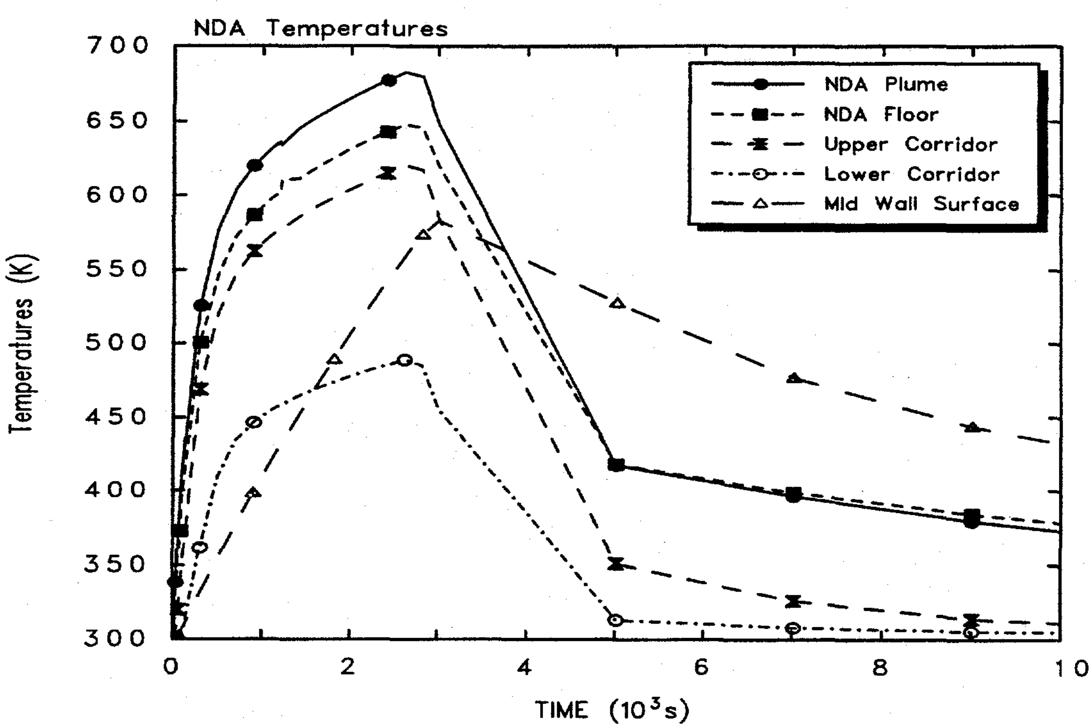

Fig. 8. NDA Laboratory Temperatures.

The flow through the towers first relieved the building pressure during the fire heatup of gases and then allowed air back into the facility after the fire went out and the gases cooled. The long-term natural circulation flow through the towers was on par with the leakage flow past the doors. However, flows to the towers first passed though a HEPA filter, thereby filtering those aerosols from the effluent to the environment.

Effect of Initial Aerosol Size Distribution. The effect of the initial size distribution was examined by comparing the results of Cases 2 and 3. Reducing the initial size distribution from 2-μm MMD to a 1-μm MMD increased the LPF by a factor 2.6. Although this effect will not significantly alter the study conclusions, a refined analysis should attempt to better define the initial size distribution.

Dynamic Shape Factor. The dynamic shape factor that tends to govern the rate of gravitational settling was varied between Cases 1 and 2. As gravitational settling is the dominant deposition mechanism, the dynamic shape factor was varied to determine how sensitive the results are to the accuracy of this input parameter. Although this is by no means an exhaustive examination of the sensitivity of the aerosol transport parameters, it does provide a measure of uncertainty to one of the more important transport parameters. A 20% increase in shape (i.e., ~20% reduction in the rate of gravitational settling) increased the LPF by about 30%.

Facility Air Infiltration. Apparently the most important parameter affecting the transport of aerosols from the facility was the rate of flow through the building. Note that the air infiltration rates depended on both the assumed wind velocity and the assumed leakage flow area that was specified as a width in the postulated door crack model. The product to the door crack width and the wind velocity provide a good method for comparing Cases 2, 5, 6, 7, 8, 9, 15, and 16 in Table 1.

The results range from an LPF of 10^{-7} if the building were assumed to be completely air tight to 0.05 if the door were cracked 5 mm in a 30-mph wind. However, a continuous 30-mph wind occurring over an 18-h period would be a very unlikely event and the doors are likely to close reasonably tight. The LPF for a 10-mph wind and a 0.5-mm crack width with an LPF of 10^{-4} is deemed much more realistic.

The wind gust model was used in Case 10 to illustrate the effect of aerosol transport. In certain applications, a transient wind velocity can significantly enhance the predicted transport of aerosols out of a facility by first pushing air into the building and then pulling the air back out again. The wind gust model had little effect here, primarily because of the relatively small flow area. The wind gust model in Case 10 increased the LPF by 12% over that of Case 2.

HEPA Filter Efficiency. For completeness, the HEPA filter efficiency was varied in Case 11, but because of its relative unimportance for these calculations, results varied only in the forth digit of accuracy. In some scenarios, this efficiency could become more important.

Effect of Soot Particles. The transport of PuO_2 aerosol particles would certainly be affected by smoke filling the same space. The presence of smoke typically has been neglected and the results considered conservative. The aerosol models used for the bulk of these calculations neglected soot particles associated with smoke produced by the fire. Soot particles are much lighter and therefore tend to settle slower than the same-sized PuO_2 particle, but the much larger particle density of smoke causes the soot to coagulate into substantially larger chains of particles that will settle faster than smaller particles. Soot coagulation will trap PuO_2 particles in the larger soot chains. The assumption that it was conservative to neglect smoke needed verification; therefore, calculations were run for that purpose.

Smoke aerosols were added in Cases 12, 13, and 14 for a 30-mph wind scenario and in Case 17 for a 10-mph scenario. The mass of smoke aerosols added was introduced to the calculation as a constant source over the course of the 1-h fire. Note that 10 kg of smoke corresponds to about 2.5% of the mass of combustibles.

These calculations clearly demonstrated that including smoke in the analysis reduced the predicted LPF substantially. Even a modest amount of smoke has a substantial effect. Calculation 17 represents how low the LPF can go with realistic conditions assumed. However, experimental verification to support the analytical models is missing from this analysis.

Effect of Ventilation System Models. Facility ventilation systems are an integral part of the facility; therefore, it would not be realistic to neglect their effect on aerosol transport, which was done in the initial case (Case 0). Note that Case 0 was run to provide initial insights before the input models were completed. However, should the dampers be closed, part of the ventilation system function would not work during the accident, i.e., relieving the pressure of thermally expanded gases through the towers. The building pressures predicted in Case 0 are shown in Fig. 9. The pressure peaked at 20 in. of water about 5 min into the fire and then decreased to subatmospheric pressures after the fire went out. Given this situation, aerosols would be driven from the building as the pressure is relieved through infiltration pathways, resulting in a higher LPF. Also, if this situation existed, the timing of container failure and the subsequent release of aerosols into the laboratory would become much more important.

The effect of the pressurization on the aerosol transport is shown by comparing the LPFs for Case 1 and Case 0 as shown in Fig. 10. Including the ventilation model reduced the LPF from 0.007 to 0.003 by eliminating the early burst released in Case 0 that was caused by building pressurization. Keeping the dampers open, thereby allowing the facility to vent to the towers through the HEPA filters, reduces the LPF.

CONCLUSIONS

The transport of respirable PuO_2 aerosols from the facility to the environment following a postulated 1-h fire in the main floor NDA laboratory depends most strongly on parameters that affect the rate of air infiltration into and out of the building, specifically infiltration flow areas and wind velocities. It is important that the building doors to the outside be closed before a postulated release of PuO_2 aerosols into the building atmosphere because open doors on opposite sides of the building could result in a rather large fraction of the aerosols being transported to the environment. This is illustrated by comparing the calculations that varied either the postulated wind velocity or the width of the cracks in the door crack model. This study assumed all doors to the outside were closed within 5 min following the initiation of the fire, well before any container holding plutonium was postulated to fail. Note that this study did not attempt to account for infiltration other than door leakage.

When reasonably small air infiltration flow rates were modeled, the predicted LPFs were substantially less than 1%. When realistic, continuous-averaged wind velocities (< 10 mph) and tightly closing doors were assumed, the predicted LPFs were generally less than 0.01%. When infiltration was eliminated, the LPF for leakage through the HEPA filters and towers was less than 0.0001%.

These calculational results should be tempered by the fact that the postulated initial aerosol size distribution has not been firmly established and the aerosol transport results are moderately sensitive to the assumed particle-size distribution. This study focused on respirable PuO_2 aerosols, i.e., < ~3 µm, by assuming a particle-size distribution with a MMD of 2 µm and a standard deviation of 2 (~75% of this distribution was < 3 µm). Note that decreasing the MMD to 1 µm almost tripled the LPF as the smaller particles settle significantly slower than the larger particles.

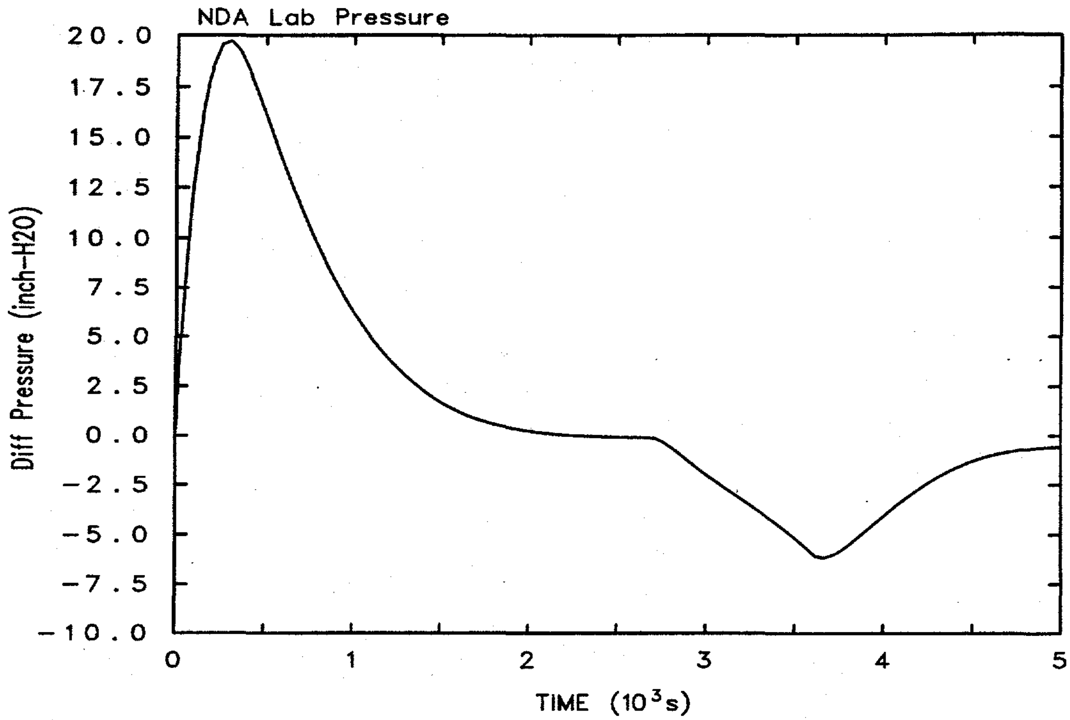

Fig. 9. NDA Laboratory Pressure (Case 0).

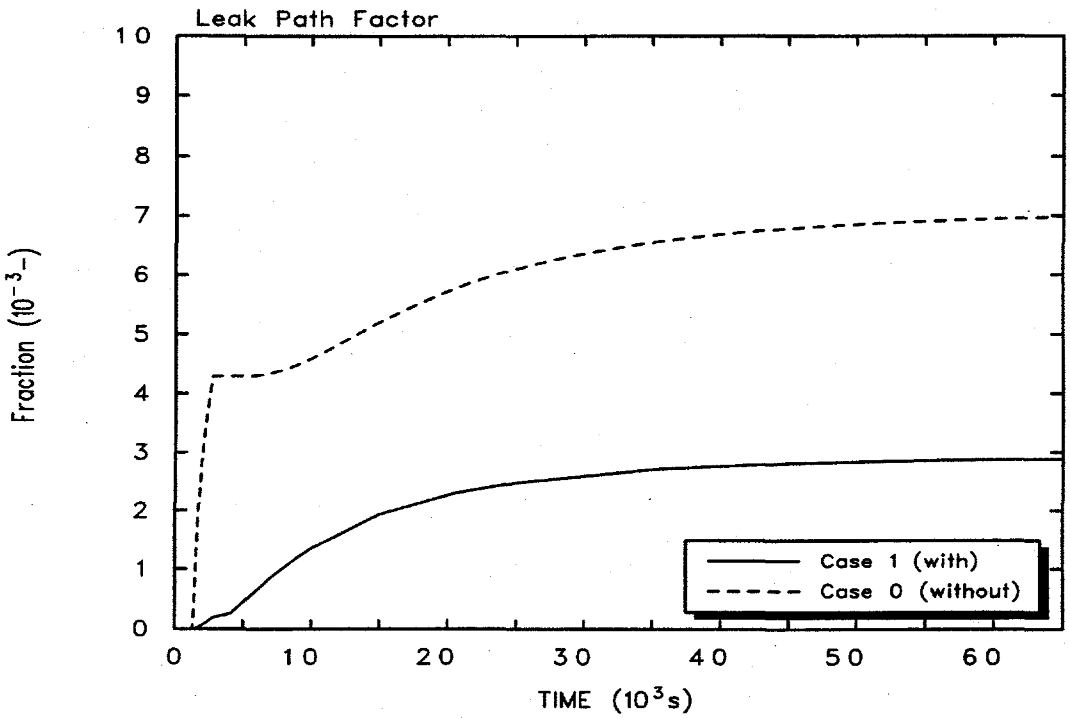

Fig. 10. LPFs With and Without Ventilation System Model.

The aerosol models used for the bulk of these calculations neglected soot particles associated with smoke produced by the fire. Soot particles are much lighter and therefore tend to settle slower than the same-sized PuO_2 particle, but the much larger particle density of smoke causes the soot to coagulate into substantially larger chains of particles that will settle faster than smaller particles. Soot coagulation will trap PuO_2 particles in the larger soot chains. Therefore, the assumption that neglecting smoke aerosols as conservative needed verification, and calculations were run for that purpose. **The calculations demonstrated that including smoke in the analysis reduced the predicted LPF substantially.** For example, assuming that 2.5% of the 864 lb of the postulated combustibles was converted to soot and entrained in the fire effluents uniformly resulted in a reduction in the LPF by over 2 orders of magnitudes.

The results were not highly sensitive to the timing of the container failure (over a range of 20 to 40 min after fire initiation) if the ventilation systems were modeled passively (fans off) and the dampers were assumed open. The open dampers prevented building pressurization from the expansion of fire-heated gases by venting these gases through the HEPA filters to either the supply or the exhaust towers. Further, the ventilation systems tended to disperse the aerosol throughout the building and ventilation ducts. If these dampers were closed so that the building was isolated from HEPA filters and towers, the building would pressurize because of the fire-heated gases, which in turn would force aerosols from the building through infiltration pathways (illustrated in Case 0).

The transport of PuO_2 aerosols was shown to be relatively insensitive to a number of input parameters and modeling considerations. These considerations included the modeling of wind gusting and the accuracy of the assumed HEPA filter efficiency.

Improved accuracy in the predictions of LPFs depends on better data for building infiltration, initial PuO_2 aerosol-size distributions, meteorological conditions, and smoke produced by the fire. Realistic modeling of these parameters potentially could reduce the predicted LPFs by orders of magnitude.

REFERENCES

1. Derek Gordon, "Nuclear Materials Storage Facility: Facility Design Description," LA-CP-98-110, April 21, 1998.

2. R. M. Summers et. al., "MELCOR Computer Code Manuals," Volumes 1 and 2, Sandia National Laboratories report SAND93-2185, NUREG/CR-6119 (September 1994).

3. C. A. Buchsted et al., "Nuclear Aircleaning Handbook," Energy Research and Development Administration report ERDA-7621 (March 1976).

4. R. D. Peacock et al., "CFAST, the Consolidated Model of Fire Growth and Smoke Transport," National Institute of Science and Technology Technical Note 1299 (1991).

5. ASHRAE Handbook: 1981 Fundamentals, Published by the American Society of Heating, Refrigerating, and Air-Conditioning Engineers, Inc., Fourth Printing (1983).